Combustion and Thermal Development of a Heavy-Duty Hydrogen IC Engine

John Hughes[1], Richard Penning[1], Ray Sullivan[1], David Bell[2], Jan Hynous[2], Charles Turquand D'Auzay[2]

[1] Ricardo UK, Shoreham Technical Centre, Shoreham-by-Sea
[2] Realis Simulation Ltd., Building 50, Shoreham Technical Centre, Shoreham-by-Sea

Abstract. Hydrogen has been identified as a promising decarbonization fuel in internal combustion engine (ICE) applications in many areas including heavy-duty on and off road, power-generation, marine, etc. Hydrogen ICEs can achieve high power density and very low tailpipe emissions. However, there are challenges; designing systems for a gaseous fuel with its own specific mixing, burn rate and combustion control needs, which can differ from legacy products. Characterisation and elimination of hot spots within the combustion are key to preventing unwanted pre-ignition.

The primary pollutant of concern for Hydrogen ICEs is NOX and this can be addressed by running the engine at very lean equivalence ratios and the use of Exhaust Gas Recirculation (EGR). Computation Fluid Dynamics (CFD) is a valuable tool to model the combustion characteristics under different conditions and can also be used to predict thermal loading.

Being able to determine thermal distribution and temperatures of the power cylinder components has always been critical to the design and development of ICE programmes. This remains a key requirement when considering hydrogen as an alternative fuel for both clean sheet hydrogen ICE designs and implementation of fuel conversions. Significant improvements have been made in recent years in the speed and accuracy of CFD tools for combustion and thermal prediction, but these still present lead times that can preclude their use in early concept work or parametric studies.

A recently developed thermal Finite Element (FE) tool helps to reduce CFD and thermal survey costs, complementing these approaches to make the engine development cycle more efficient. This new FE based tool meets the current and future challenges of ICE design and development, to accurately predict the thermal loading and temperatures of an ICE quickly under multiple full-load and part-load conditions, relevant for hydrogen combustion development.

This paper presents how both CFD and the FE analytical tools are applied to a Euro VI HD engine converted to operate on hydrogen gas using direct injection. A CFD model is presented that accurately predicts the trends in engine performance and correctly captures the flame acceleration driven by thermo-diffusive effects. In addition, CFD combustion and FE temperature results are presented at low-, part and full-load conditions including a lambda swing to investigate the effect of different equivalence ratios on structural temperature. These data are compared with measurements taken from a single-cylinder engine tested at the Ricardo hydrogen test facility.

Keywords: Hydrogen, Combustion, Thermal, Heavy-Duty, CFD, FE, ICE

1 Introduction

Hydrogen is increasingly considered a key energy carrier in the transition to a net zero carbon economy. Hydrogen-fuelled internal combustion engines have the advantage of building on proven, robust, and cost-effective technologies [1,2]. Hydrogen ICEs are also tolerant to fuel and intake-air contamination, and their thermal management is relatively straightforward [3,4,5].

In this research work Ricardo have investigated a direct-injection (DI) hydrogen combustion system. Direct injection provides greater flexibility for injection strategies, improves volumetric efficiency, allows lower boost pressures to be used, and reduces the presence of hydrogen in the intake manifold, minimising the risk of backfire compared to port fuel injection (PFI). The programme began with a single-cylinder research engine [6,7], before continuing with a six-cylinder engine. This paper presents results from both engines.

The multi-cylinder engine work reported is part of the HIMET (Hydrogen in an Integrated Maritime Energy Transition) project [8], which is itself an element of the Clean Maritime Demonstration Competition [9]. The maritime application (a small island ferry) has guided the approach taken to operating conditions and emissions control, but the engine itself is also suitable for on-highway and off-highway heavy-duty applications.

The primary pollutant of concern for hydrogen ICEs is NOx which can be addressed by running the engine at very lean equivalence ratios and the use of Exhaust Gas Recirculation (EGR). [10] presented in detail how CFD can be used to model hydrogen combustion under different conditions and proposed a methodology to account for thermo-diffusive instability, which manifests itself at lean charge conditions, using a flame speed table modified with novel correlations extracted from high-fidelity numerical simulations.

Being able to determine the thermal distribution and temperatures of the power cylinder components has always been critical to the design and development of ICE programmes. This remains a key requirement when considering hydrogen as an alternative fuel for both clean sheet hydrogen ICE designs and implementation of fuel conversions. [11] presented in detail how an extended analytically FE-based tool can be used to predict thermal loading of hydrogen ICEs.

2 Key Engine Features

The research engines have been developed from a Euro VI heavy-duty Diesel and natural gas engine designs, converted to run on hydrogen fuel. Key engine specifications are listed in Table 1.

Table 1. Engine Specifications

	Single-Cylinder Engine	Multi-Cylinder Engine
Bore [mm]	131	130

Stroke [mm]	158	160
Cylinders	1	6
Swept Volume [L]	2.1	12.7
Compression Ratio	12.6:1	11.9:1
Rated Power Speed [rev/min]	1800	1800
Piston and Bottom End	Diesel piston with modified bowl	CNG engine piston
Cylinder Head	Production CNG unit head modified for DI hydrogen	
Injection system	IGBT inductive coils 103 mJ maximum ignition energy	
Fuel Injection System	Direct Injection	Direct injection Twin port injection
Fuel Pressure [bar]	35	35 (DI) 12 (PFI)
Boost System	Testbed system	Variable-geometry turbocharger (VGT)
EGR	Testbed cooled EGR system	Cooled HP EGR

Concept development for the engines has been described in previous publications [6,7]. In many areas the baseline engine designs were retained, including the flat cylinder head and swirl port combustion system. CNG engine unit cylinder heads were modified to incorporate BorgWarner DI-CHG 6.2 direct hydrogen injectors, as shown in Figure 1.

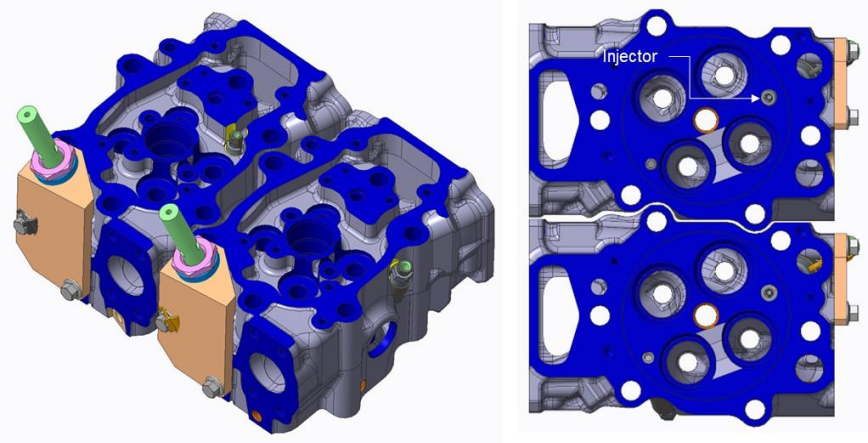

Fig. 1. Unit cylinder heads with direct hydrogen injector installation

For the single-cylinder engine (SCE), a production diesel piston was modified to reduce the compression ratio, as shown in Figure 2. For the multi-cylinder engine (MCE), a production CNG piston was used.

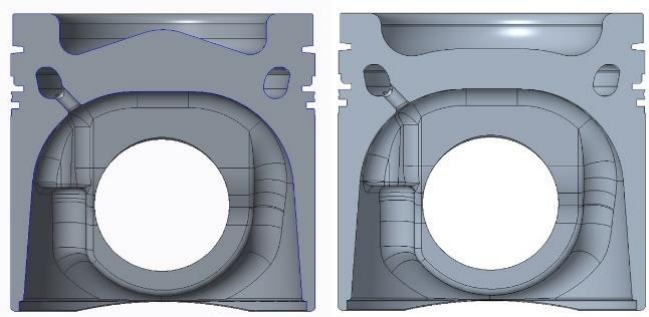

Fig. 2. Production Diesel piston (left) and modified piston for SCE hydrogen application (right)

The testbed installations for the single-cylinder engine at the University of Brighton, and for the multi-cylinder engine at Ricardo, are shown in Figure 3.

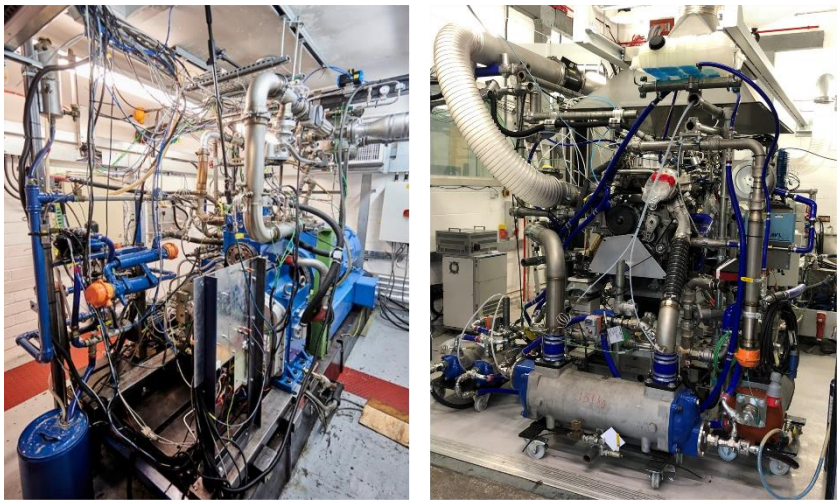

Fig. 3. Single-cylinder engine (left) and multi-cylinder engine (right) testbed installations

3 Test Results

3.1 Impact of Air-Fuel Ratio on Combustion

The lean limit was at λ 4.5 or higher for all the load conditions and it was possible to run with stoichiometric mixture at 3.5 and 9 bar GIMEP. Figure 4 illustrates the impact load and lambda have on combustion. At lower lambda values the CoV of GIMEP starts to rise as abnormal combustion becomes an influence. At lambda values between 1.5 and 4.0 combustion duration (10 – 90% MFB) is relatively constant with load. As lambda exceeds 4.0 there is more slowing of burn-rates at lower load.

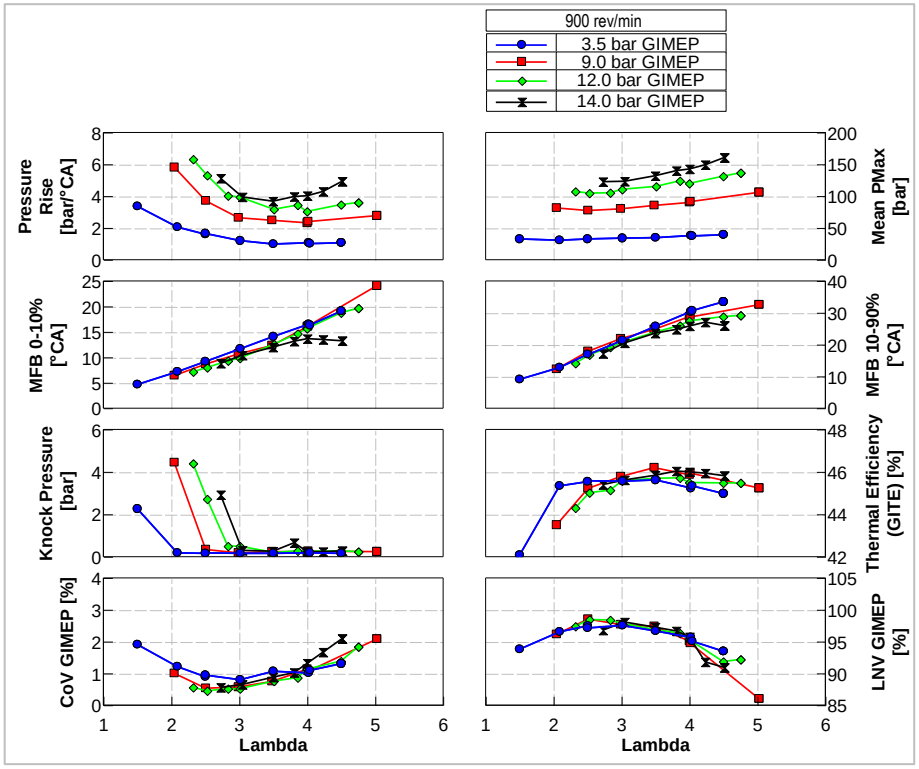

Fig. 4. Single-cylinder engine (left) and multi-cylinder engine (right) testbed

The relationship between abnormal combustion and load and lambda is very evident. As load increases the lowest air-fuel ratio that can be achieved without knock also increases. At 3.5 bar GIMEP, abnormal combustion was observed for lambda below 2.0, whereas at 14 bar GIMEP lambda values below 3.0 resulted in knock and abnormal combustion events occurring. Overall, as load increases there is a narrowing of the lambda range that can be utilized. At lower lambda knock and abnormal combustion are the limitation. At the lean end there is a deterioration in combustion stability.

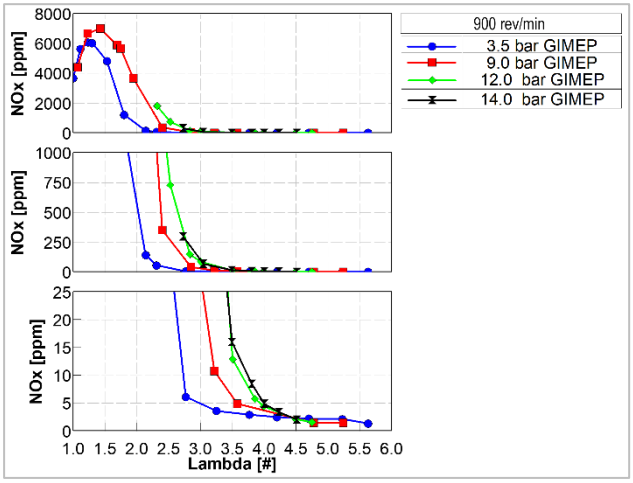

Fig. 5. Lambda sweep engine-out emissions at 900 rev/min, 0% EGR, 3.5, 9.0, 12.0 and 14.0 bar GIMEP

Figure 5 shows the characteristic relationship between NOx emissions and air-fuel ratio. Peak NOx emissions of 6600 and 7000 ppm were observed at 3.5 bar GIMEP, λ 1.3 and at 9.0 bar GIMEP, λ 1.4 respectively. NOx values then drop rapidly as lambda is increased and combustion temperatures cool. Further testing at higher speeds showed NOx formation to be more dominated by load than speed.

3.2 Impact of EGR on Combustion

As expected EGR dilution slows combustion and the rate of pressure rise but leads to increased cylinder pressures due to increased trapped mass. At higher loads the ability to tolerate lean combustion or large amounts of EGR may be superseded by cylinder pressure limitations, especially in retrofit applications. The added EGR also allows for the engine to be de-throttled as intake manifold pressure crosses barometric pressure at approximately 40% EGR. The ability to tolerate a large amount of EGR presents another option to reduce pumping losses.

The high EGR rate considerably increases the specific heat capacity of the system hence lowering combustion temperatures and reducing the rate of NOx formation.

3.3 Ignition Timing Optimisation

The ability to select the ignition timing for best efficiency is limited by both abnormal combustion and by NOx emissions. NOx formation increases as ignition timing is advanced due to higher in-cylinder temperatures; hence advancing ignition timing at λ 2.0 produces a greater increase in NOx emissions than at the leaner conditions. At λ 2.5 and 3.0 slower combustion also means the rate of pressure rise reduces resulting in cooler combustion system and lower NOx emissions.

The optimum efficiency for these swings is found between 2 and 5.5 °CA ATDC(F) which is advanced compared to spark-ignited gasoline engines. Other swings show

similar tendencies but are also influenced by relative speed, load, EGR rate, etc. At higher speeds and loads (1800 rev/min, 14 bar GIMEP) relatively advanced ignition timing can be tolerated compared to stoichiometric gasoline engines, which have more retarded combustion phasing due to knock.

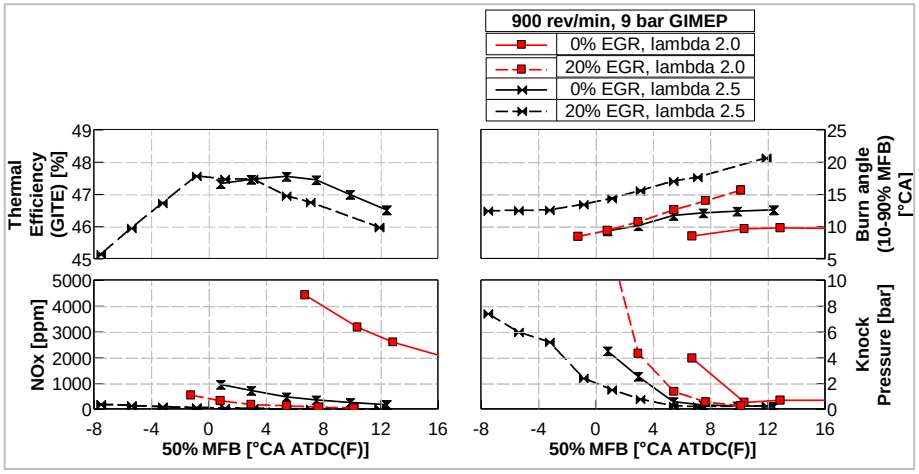

Fig, 6. Ignition timing swings for 900 rev/min, 9 bar GIMEP at different air-fuel ratio and EGR rates

Figure 6 shows ignition timing optimisation with and without EGR. The addition of EGR delays the onset of knock and once knock is encountered reduces its amplitude. EGR is also very effective at reducing the rate of NOx formation but there is a trade-off with efficiency if ignition timing cannot be fully optimised.

Start of injection (SOI) was also investigated to determine the impact of air-fuel mixture homogeneity on combustion and emissions. Four swings have been selected to illustrate the characteristics observed during this study.

As the injection timing is swept from the most advanced setting of 300 to 180 °CA BTDC(F) an increase in NOx formation is observed. This increase is matched by a reduction of burn angles (10-90% MFB), as well as increases in rate of pressure rise and maximum cylinder pressure.

Combustion stability is also influenced by the injection timing. As SOI is retarded to <240 °CA the CoV GIMEP starts to increase and the LNV GIMEP decreases. Also of note is the fact that at 1800 rev/min, 9 bar GIMEP λ 2.5 the system is very close to its knock threshold. As injection timing is retarded this becomes more evident and increasing knocking pressures were measured.

Overall, the data suggests that the air-fuel mixture is not fully homogeneous even at very advanced injection timings.

3.4 Abnormal Combustion

The ignition timing swings presented earlier show that conventional end-gas knock is observed, which can be moderated with retarded ignition timing. In addition to this

predictable behaviour there are also occurrences of extreme abnormal combustion events that are much less predictable.

Test showed multiple instances of knock, single and multiple pre-ignition events across different calibrations. Figures 7 and 8 show examples of some of the phenomena observed.

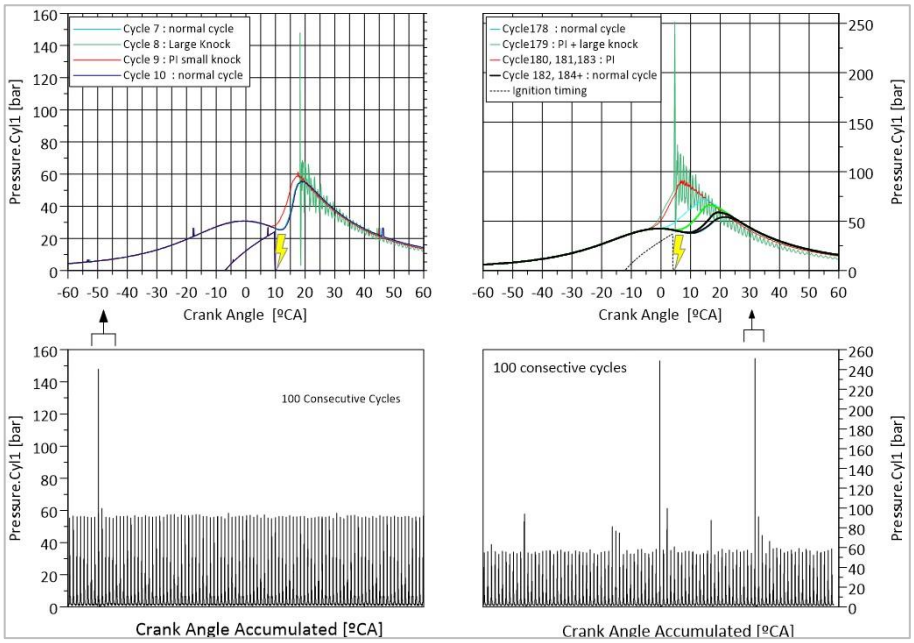

Fig. 7. Examples of the stochastic nature of more extreme abnormal combustion. Left: Large single knock event followed by single PI event. Right: PI with large knock event followed by multiple smaller PI events

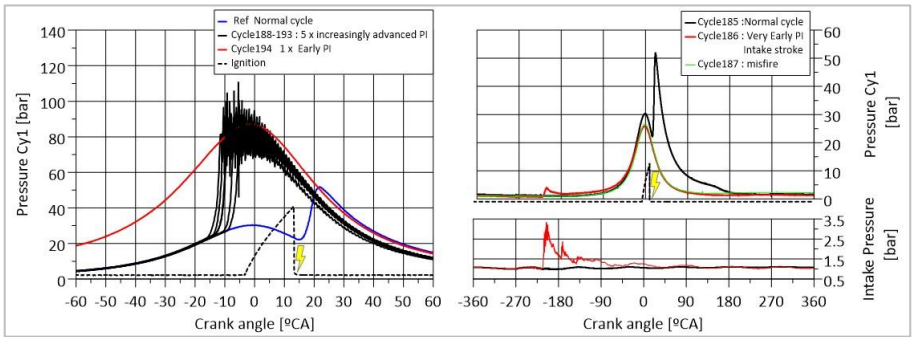

Fig. 8. Left: PI progressively advanced with each cycle, followed by a very early PI event. Right: Single PI event during intake stroke (upper) with pressure wave registering on the intake pressure transducer (lower)

Abnormal combustion in hydrogen engines is a complex combination of pre-ignition, end-gas knock, and backfire. Hot spots, oil droplets and oil-derived particles, and ignition system characteristics, are all likely to be involved in the nucleation of these events. As a result, the mitigation of abnormal combustion requires a complete system approach to hydrogen engine design, simulation, development, and calibration.

4 Engine Simulation

The experimental data described has been used to validate 1-D and 3-D simulation models of the engines. These models allow different operating scenarios to be explored in parallel with engine testing.

4.1 1-D Performance Simulation

1-D gas-dynamic models of each engine were created using Realis WAVE software and validated against engine test data as indicated in Figure 9.

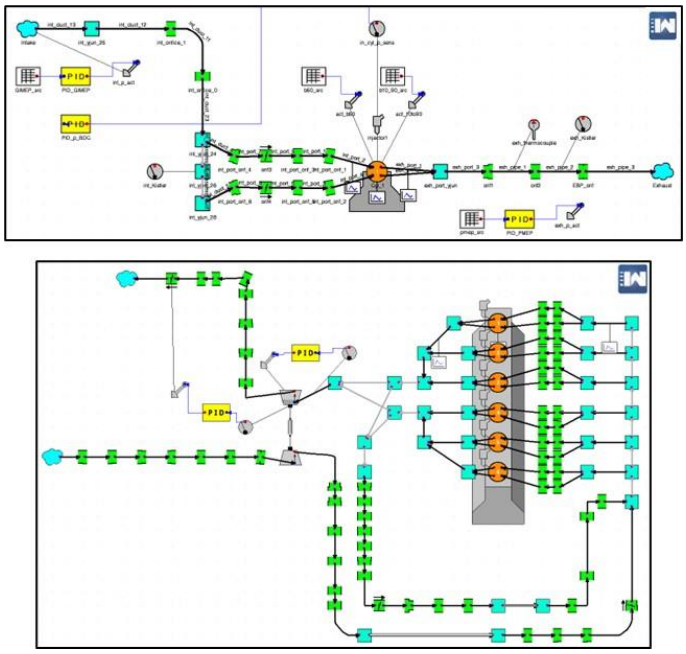

Fig. 9. 1-D WAVE models of single cylinder (upper) and multi-cylinder (lower) hydrogen engines

The 1-D models have been used for the development of a predictive Hydrogen Combustion Duration Sub-model (HCDS), as shown in Figure 10. HCDS is a semi empirical sub-model based on the combination of laminar and turbulent flame speed calculation and empirical test data. HCDS reflects in-cylinder conditions such as lambda, pressure, amount of internal and external residuals etc. The sub-model also reacts to the change

of bore, stroke, and intake port design. HCDS is under continuous development following the progress of the engine test programme to support the future development of hydrogen combustion engines.

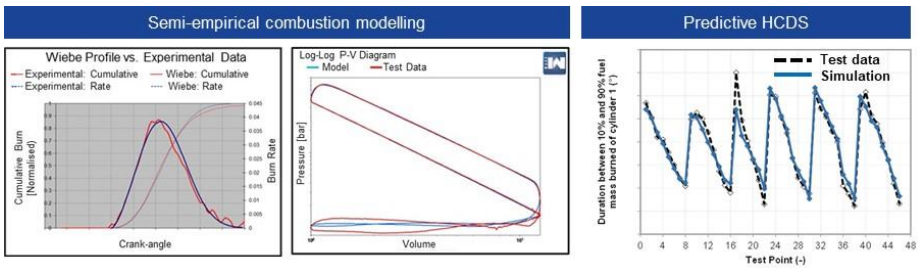

Fig. 10. Hydrogen combustion duration sub-model (HCDS)

4.2 3-D CFD Simulation

A well-defined process exists for combustion system development using in-cylinder CFD and conventional fuels, as shown in Figure 11. When considering hydrogen as a fuel for engines the same general approach can be employed although some modification is required.

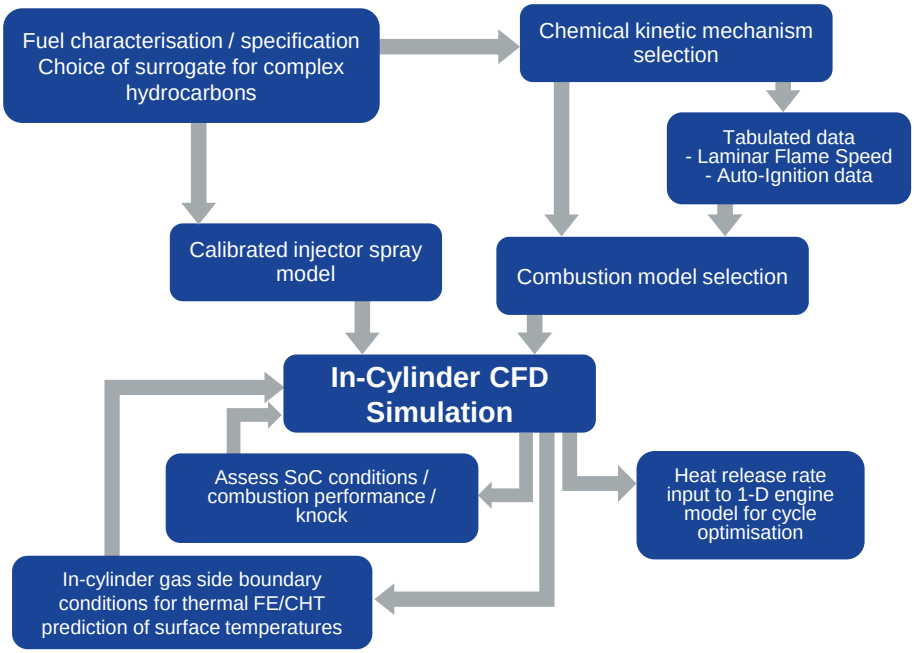

Fig. 11. Overall process for 3-D CFD simulation

Fuel characterisation, choice of surrogates and chemical kinetic mechanism becomes much simpler as hydrogen has a simple composition with known properties and a limited number of reactions that need to be considered. However as presented previously [12] the flame speed behaviour of H_2 is very different to other fuels and existing flame speed models require adaptation.

For fuel and air mixing, the practice of modelling traditional liquid fuel sprays is also well established with a discrete droplet Lagrangian approach. It might be thought that the single-phase nature of H_2 injection into air would be relatively simple in comparison to liquid fuel injection, however the very large velocities and complex behaviour of the under-expanded jet need to be captured directly by the flow solver which increases the computational requirement.

When interpretating simulation results, established targets exist for mixture homogeneity with traditional fuels. These need refinement for H_2 as on one hand it is very diffusive and therefore mixes faster and on the other combustion shows increased sensitivity to variation in air-fuel ratio.

Lastly existing knock models may not be applicable to H_2 due to the relatively high charge pressures and temperatures before the start of combustion from the high boost levels required for lean operation.

Data from the experimental engines has been used to validate updated hydrogen combustion CFD models. The Realis VECTIS software includes the thermo-diffusive instability effects and a general methodology for the prediction of hydrogen combustion [10].

Concept level in-cylinder CFD simulations of the SCE were revisited and refined. Two main enhancements were made to the modelling: the H_2 injection was validated for the final injector configuration and the combustion simulations employed the developed enhanced models for lean hydrogen combustion.

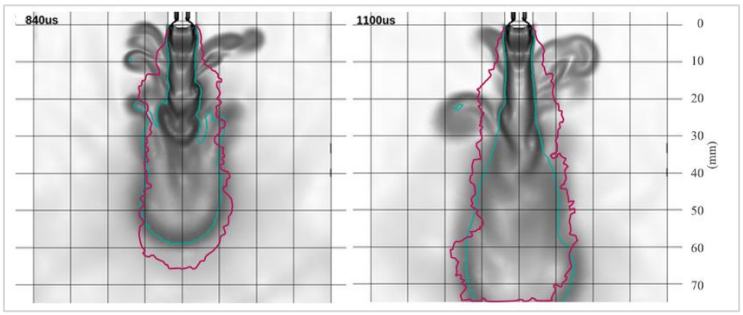

Fig. 12. Comparison of experimental data [12] indicating the outline of the injection jet (in magenta) with simulation results of the local pressure gradient, and an outline contour marking the extent $Y_{CH4} = 0.1$ (cyan)

A three-point lambda swing was considered at 1400 rev/min and 9 bar GIMEP with nominal lambdas of 2.5, 3.0 and 3.5. A relatively early start of injection timing was used during testing to try an ensure as close to a homogeneous mixture as possible at spark timing. Figure 12 shows an example of the spray match for the injector used in the SCE for injection of CH_4.

The validated spray model was then incorporated into the full in-cylinder simulation allowing the interaction of the fuel spray and intake charge to be captured more faithfully and the evolution of the mixing to be assessed. Figure 13 shows that the H_2 mixes rapidly with the probability distribution curve rapidly becoming narrower during compression. However as shown in the accompanying image the mixture is not full homogeneous.

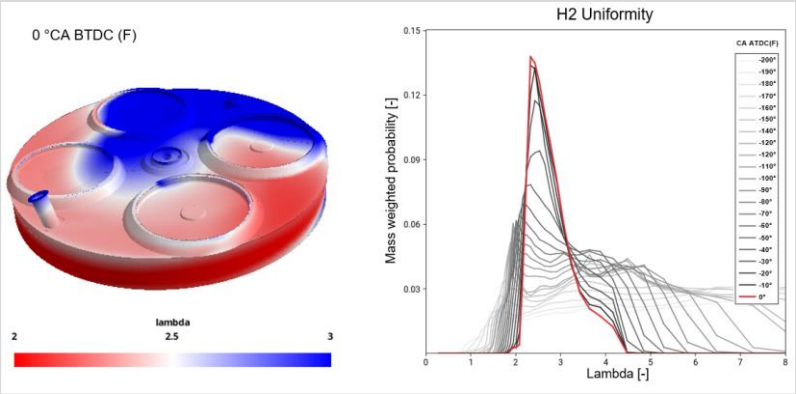

Fig. 13. Hydrogen distribution at TDC(F) and mass weighted H_2 distribution probability during compression for the λ 2.5 key point

With trapped conditions at spark timing now matched to the measured test points the combustion prediction can now be more fairly assessed. Both the standard combustion approach and the enhanced lean hydrogen combustion model were evaluated. The two models were tuned to match the test data at the mid, λ 3.0, test point of the three-point test swing before being run at the two other test points without further tuning. Figure 14 shows the response of the models to a change in lambda. The match achieved when tuning the models at the mid-point is very good, with both models lying on the test pressure curve. As the operating lambda is changed the standard model tends to undershoot the measured pressure at the richer condition and overshoot at the leaner condition. With the new thermo-diffusive model, the response is significantly improved.

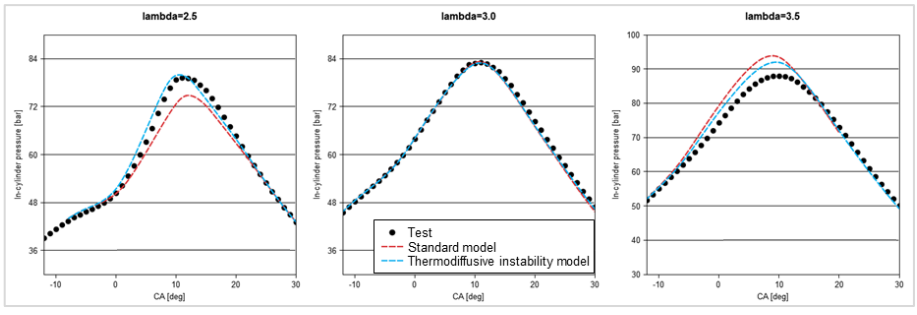

Fig. 14. Predicted in-cylinder pressure compared to test for three-point lambda swing

With additional data from the SCE the combustion model validation was extended to higher loads. The higher load cases considered were a lower speed 900 rev/min, 18 bar GIMEP running at λ 2.8 and a higher speed 1800 rev/min, 14 bar GIMEP point at λ 2.6. The same process was used as in the previous cases, with the simulation firstly considering the intake event with injection to establish trapped conditions, air motion and fuel mixing before then continuing with combustion. The new thermo-diffusive combustion model was used with the same parameter settings as found in the initial model tuning at 1400 rev/min, 9 bar GIMEP.

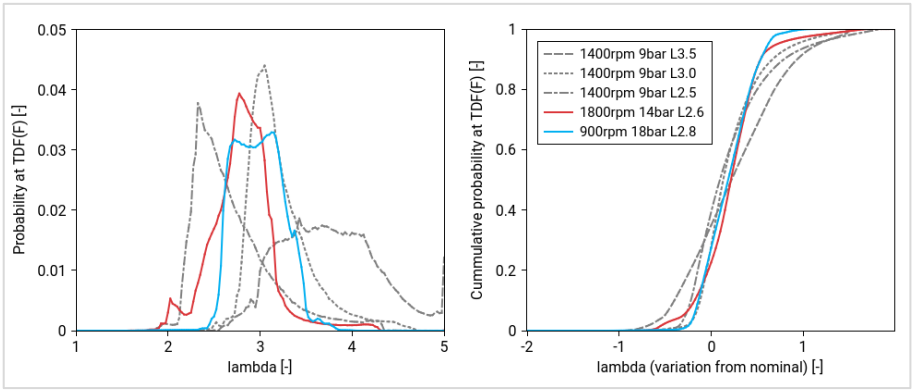

Fig. 15. Comparison of mixture homogeneity at TDC(F) for different operating points

The start of injection timing (-280°CA ATDC(F)) was the same for the different operating points simulated. The overall mixing was very similar for the different cases, as shown in Figure 15 above, despite the change in fuelling quantity, and therefore injection duration, and with the different engine speed. This suggests that the engine architecture and layout play a significant role in the fuel preparation behaviour.

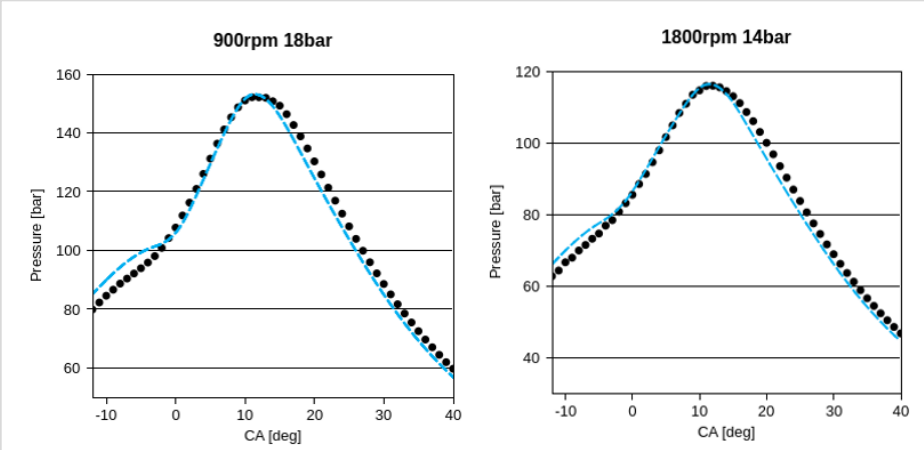

Fig. 16. Predicted in-cylinder pressure compared to measurements at higher loads

The higher load cases considered were a lower speed 900 rev/min, 18 bar GIMEP running at λ 2.8 and a higher speed 1800 rev/min, 14 bar GIMEP point at λ 2.6. The predicted combustion gave a good match to the measured test data without requiring additional tuning as shown in Figure 16.

Ongoing and future work will be to verify the combustion model prediction with and without EGR, and to study abnormal combustion events such as pre-ignition (PI) and knock.

4.3 3-D FE Thermal Simulation

The Realis FEARCE-Vulcan software calculates the thermal boundary conditions of all the components of a hydrogen ICE power cylinder using physical models and semi-empirical correlations. An iterative solution is used that captures all the heat paths in detail where each solution runs fast enough to allow different design variants to be assessed quickly for multiple operating conditions. This software tool has been extended to for hydrogen-fuelled engines [11]. The predictions from this software tool are compared with measurements on the SCE.

A set of comprehensive thermal survey measurements were performed on the SCE for a range of low-, part- and high-load steady-state conditions, with a sweep of λ from 1.0 to 5.0. [11] presented in detail the validation of FEARCE-Vulcan using those measurements. In this paper the authors present a subset of those results, presenting data for λ between 2.0 and 3.5.

The cylinder head was instrumented with shielded ground K-type thermocouples as shown in Figure 17.

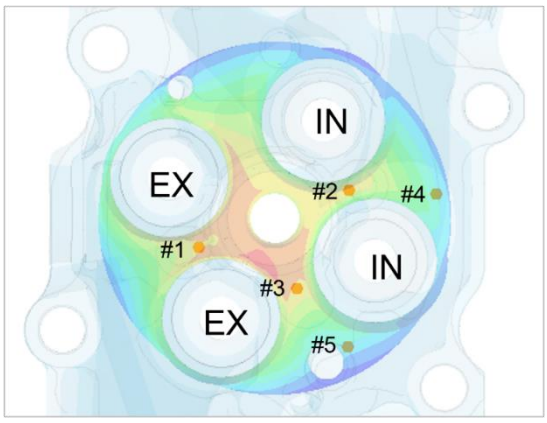

Fig. 17. Cylinder head thermocouple locations

Figures 18 to 22 show at each thermocouple location the measured and predicted temperatures with increasing load and speed, and at each speed/load condition a nominal lambda sweep from 2.0 to 3.5.

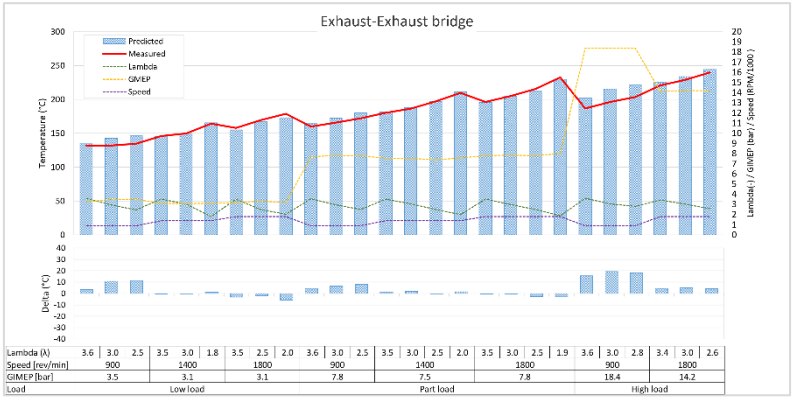

Fig. 18. Measured and predicted temperatures at the exhaust-exhaust valve bridge (#1)

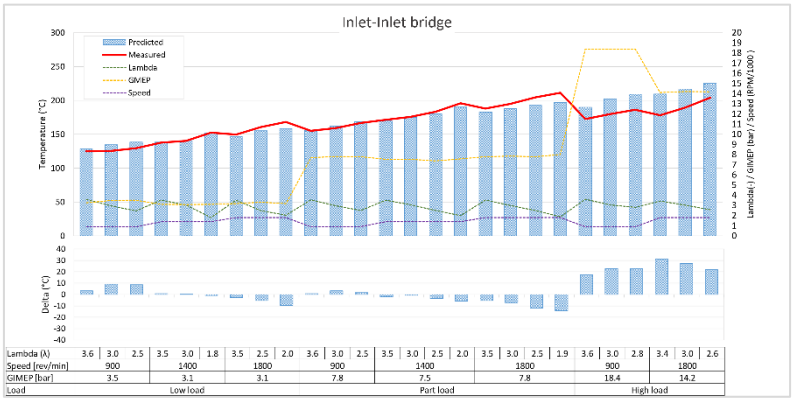

Fig. 19. Measured and predicted temperatures at the inlet-inlet valve bridge (#2)

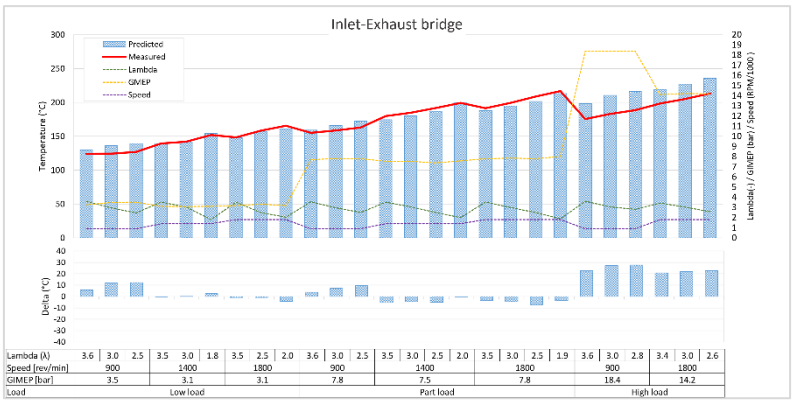

Fig. 20. Measured and predicted temperatures at the inlet-exhaust valve bridge (#3)

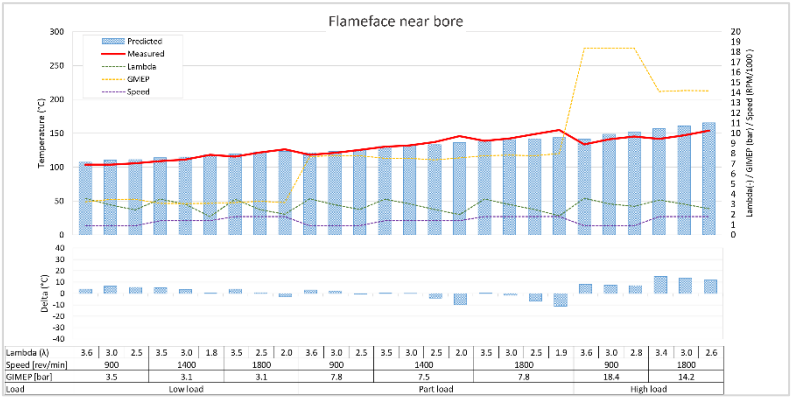

Fig. 21. Measured and predicted temperatures on the flame-face near the bore (#4)

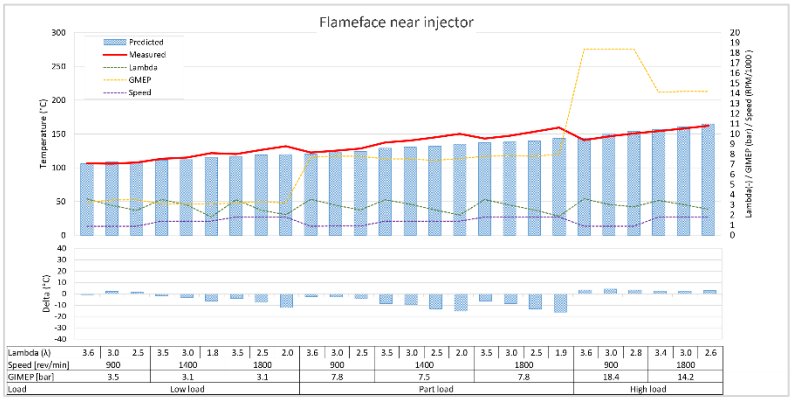

Fig. 22. Measured and predicted temperatures on the flame-face near the injector (#5)

These figures show that at each engine speed/load condition the metal temperatures decrease with increasing lambda (right to left in the figures) as combustion temperatures cool. The figures also show excellent agreement of the predicted results against measurement both in terms of trend and absolute values. At all the locations most test points are within 10 °C and all are within 20 °C except for some data at high load at the inlet-inlet and inlet-exhaust bridges where the temperatures are over predicted. This validated dataset shows that the tool can be used predict temperatures with confidence and that those temperatures can be used as input to assess the durability of the cylinder head, piston, and cylinder block for hydrogen-fuelled engines.

In this study the heat transfer from the in-cylinder gas to walls was calculated using the Woschni correlation [13]. The applicability of this correlation to hydrogen modelling has been a subject of several investigations, including [14]. Ongoing and future work will look at using the Hohenberg correlation [15], in part to investigate whether the poorer correlation at high load can be attributed to the HTC correlation.

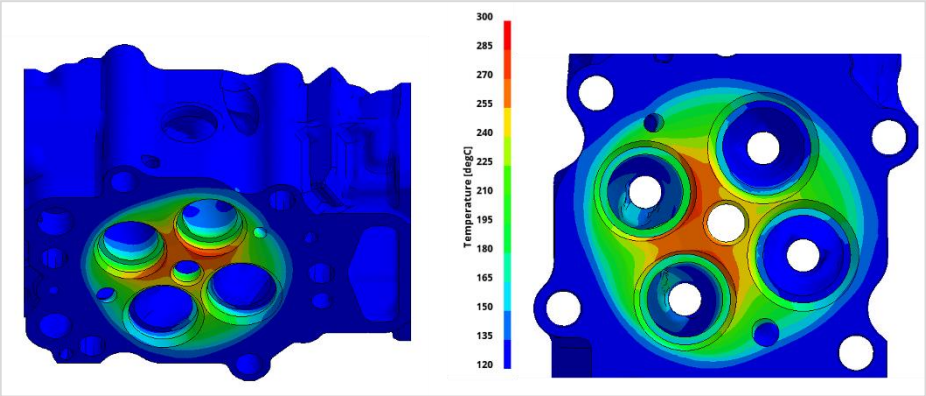

Fig. 23. Predicted cylinder head temperatures at 1800 rev/min 14.2 bar λ 2.6

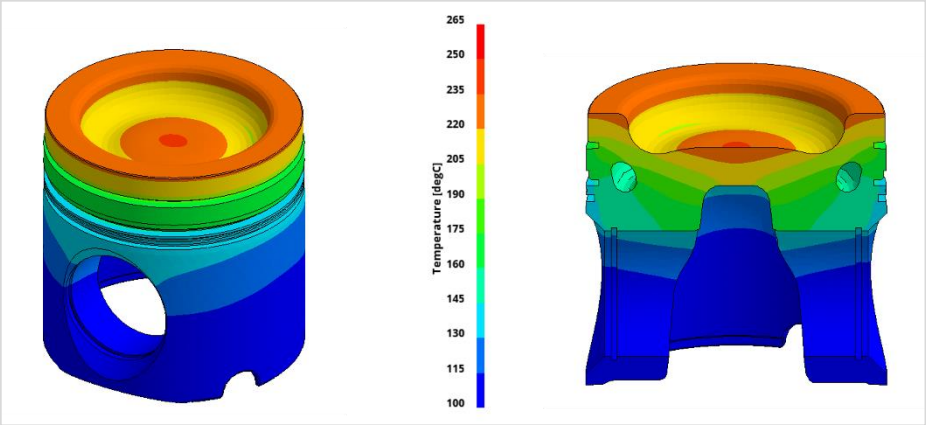

Fig. 24. Predicted piston temperatures at 1800 rev/min 14.2 bar λ 2.6

Figures 23 and 24 show the predicted temperatures on the cylinder head and piston at the highest thermal loading, 1800 rev/min 14.2 bar λ 2.6. The peak temperatures are below 250 ^{o}C, which is the accepted guideline for ensuring low-cycle structural durability of aluminium cylinder heads and piston that operate with hydrocarbon fuels. However, further work is required to fully understand possible localised high structural temperatures arising from the high energy release associated with hydrogen combustion, in particular abnormal combustion presented earlier. This requires further testing, instrumenting the piston with templugs or thermocouples, together with simulation to help understand whether the unique characteristics of hydrogen combustion is likely to impact the durability of cylinder components.

Ongoing and future work will apply this presented software tool to predicted temperatures on the multi-cylinder engine to assess the durability of the cylinder head, piston, and cylinder block.

5 Conclusions

- The authors have developed single-cylinder and multi-cylinder heavy-duty hydrogen engines, which employ direct fuel injection and spark-ignition combustion.
- The combustion systems developed have high dilution tolerance, with lean limits extending to lambda 5.5 and EGR rates beyond 40%.
- Operating at lambda 3, engine-out NOx levels are below 10 ppm for the multi-cylinder engine, which means that IMO Tier 3 emission limits can be achieved without NOx aftertreatment.
- Abnormal combustion is a constant feature of hydrogen combustion, and its mitigation requires a complete system approach to engine design, development, and calibration.
- The simulation toolset has been updated for hydrogen engines, including a hydrogen combustion duration sub-model (HCDS) for 1-D simulation, an extended FE based thermal analysis tool to assess structural temperatures for hydrogen fuelled engines and a comprehensive review and development of the tools and processes needed for 3-D CFD simulation.

References

1. Stockhausen, W., Natkin, R., Kabat, D., Reams, L. et al.: *Ford P2000 Hydrogen Engine Design and Vehicle Development Program*, SAE Technical Paper 2002-01-0240, 2002, https://doi.org/10.4271/2002-01-0240.
2. Berckmüller, M., Rottengruber, H., Eder, A., Brehm, N. et al.: *Potentials of a Charged SI-Hydrogen Engine*, SAE Technical Paper 2003-01-3210, 2003, https://doi.org/10.4271/2003-01-3210.
3. Thomas Pauer, Heiko Weller, Erik Schünemann, Helmut Eichlseder, Peter Grabner, Klaus Schaffer: *H_2 ICE for Future Passenger Cars and Light Commercial Vehicles*. International Vienna Motor Symposium, 2020.
4. G. Maio et al: Retrofitting A Diesel Baseline To A Fully Ha Spark Ignition Engine By Combining Experiments, OD/1D, And 3D CFD Simulations: 31st Aachen Colloquium Sustainable Mobility 2022. October 10-12, 2022.
5. Dr. Yohan Chi, et al.: *Hydrogen Internal Combustion Engine: Zero- Impact Emission Technology for Sustainable Mobility*. 31st Aachen Colloquium Sustainable Mobility 2022. October 10-12, 2022.
6. Atkins, P. A., N. Fox, A. Saroop, J. Hughes, N. Coles, T. Downes, A. Thurston: *Examining Trade-Offs Between NOx Emissions and Hydrogen Slip For Hydrogen Combustion Engines*, THIESEL 2022 Conference on Thermo- and Fluid Dynamics of Clean Propulsion Powerplants. 13-16 Sept 2022.
7. John Hughes, David Bennet, Angela Loiudice, Nicholas Coles, Trevor Downes, Agam Saroop, Richard Penning, Lukáš Valenta, Peter Rabanser, Jonathan Davis, Jackson Harvey-Bush, Alvaro Concepcion Calero, Richard Osborne, Penny Atkins, Roger Allcorn, Nigel Fox. *Assessment of a Direct-Injection, Spark-Ignited, Hydrogen-Fuelled Heavy-Duty Engine.* 17th International MTZ Conference on Heavy-Duty Engines. 16-17 Nov 2022, Donaueschingen, Germany.
8. Ricardo plc: Ricardo Works with UK Consortium to Accelerate Maritime Decarbonisation in Orkney. Press release, 15 September 2021.

9. Department for Transport and Innovate UK: *Multi-year Clean Maritime Demonstration Competition*. https://www.gov.uk/government/publications/clean-maritime-demonstration-competition-cmdc Accessed 31st May 2023.
10. Hernandez, I., Turquand d'Auzay, C., Penning, R., Shapiro, E., Hughes, J.: *Thermo-Diffusive Flame Speed Adjustment and its Application to Hydrogen Engines*, SAE Technical Paper 2023-01-0197, 2023, doi:10.4271/2023-01-0197.
11. Bell, D., Grimley, P., Hynous, J., Shapiro, E., Osborne, R, Valenta, L. *Calculation of Thermal Boundary Conditions for Hydrogen Internal Combustion Engines*, SAE Technical Paper 2023-01-1675, 2023, doi:10.4271/2023-01-1675
12. Lazzaro, M., Catapano, F., and Sementa, P.: *Experimental Characterization of Methane Direct Injection from an Outward-Opening Poppet-Valve Injector*. SAE Technical Paper 2019-24-0135, 2019, doi:10.4271/2019-24-0135
13. Woschni, G., "A Universally Applicable Equation for the Instantaneous Heat Transfer Coefficient in the Internal Combustion Engine," SAE Technical Paper 670931, 1967,https://doi.org/10.4271/670931.
14. Tabatabaie T, Ehteram MA, Hosseini V. Investigating the effect of the heat transfer correlation on the predictability of a multi-zone combustion model of a hydrogen-fuelled spark ignition engine. Proceedings of the Institution of Mechanical Engineers, Part D: Journal of Automobile Engineering. 2016;230(1):70-81 https://doi.org/10.1177/0954407015578047
15. Hohenberg, G., "Advanced Approaches for Heat Transfer Calculations," SAE Technical Paper 790825, 1979, https://doi.org/10.4271/790825.

Glossary

ATDC(F)	After top dead centre firing
ATS	Aftertreatment systems
CA	Crank angle
CFD	Computational fluid dynamics
CHG	Compressed hydrogen gas
CNG	Compressed natural gas
CO	Carbon monoxide
CO2	Carbon dioxide
CoV	Coefficient of Variation
EGR	Exhaust Gas Recirculation
GIMEP	Gross indicated mean effective pressure
GITE	Gross indicated thermal efficiency
HC	Hydrocarbon
HCDS	Hydrogen Combustion Duration Sub-model
ICE	Internal Combustion Engine
LNV	Lower normalised value
MCE	Multi-cylinder engine
MFB	Mass fraction burned
NOx	Nitrogen oxides
PI	Pre-Ignition
PPM	Parts per million
SCE	Single-cylinder engine
TDC	Top dead centre